DOE AWARD DE-FC26-03NT41974

QUANTUM WELL THERMOELECTRICS FOR CONVERTING WASTE HEAT TO ELECTRICITY

FINAL TECHNICAL REPORT

Submitted By

Hi-Z Technology, Inc.
7606 Miramar Road, Suite 7400
San Diego, CA 92126

Prepared By

Dr. Saeid Ghamaty, P.I.
Email: Saeid@Technologist.Com
Phone: 858-952-4942

DISCLAIMER

Abstract

Fabrication development of high efficiency quantum well (QW) thermoelectric continues with the P-type and N-type $Si/Si_{80}Ge_{20}$ films with encouraging results. These films are fabricated on Si substrates and are being developed for low as well as high temperature operation.

Both isothermal and gradient life testing are underway. One couple has achieved over 4000 hours at T_H of 300°C and T_C of 50°C with little or no degradation. Emphasis is now shifting towards couple and module design and fabrication, especially low resistance joining between N and P legs. These modules can be used in future energy conversion systems as well as for air conditioning.

TABLE OF CONTENTS

LIST OF GRAPHICS AND TABLES

Introduction

Hi-Z Technology, Inc. (Hi-Z) is currently developing many different thermoelectric generator designs that are used to convert waste heat or heat sources directly to electricity. These include waste heat recovery from diesel trucks as well as automobiles and thermoelectric power generators including space application.

Bi_2Te_3 alloys, PbTe alloys, and SiGe based materials are presently used for power generation in remote locations, for example in deep space probes or direct conversion in general. However in most waste heat recovery and direct heat conversion applications an improvement in the efficiency of the energy conversion process from heat into electricity is needed. The efficiency of thermoelectric energy conversion devices is strongly limited by the performance of the materials, which is normally measured in terms of a *Figure of Merit* Z (see next section).

The breakthrough approach to increasing Z is to form compositionally modulated materials, mainly by QW confinement of carriers in the active layers in a multilayer film by adjacent barrier layers. The core concept is to enclose each electrically active layer by a material which has a band offset sufficient to form a barrier for the charge carriers. The major improvement in Z is expected to follow from an increased Seebeck coefficient that results from an increase in the density of states. There may also be a significant increase on the carrier mobility due to quantum confinement, so ideally there is an improvement in Z from the Seebeck coefficient, and the electrical conductivity. Also, the thermal conductivity, is reduced due to strain between the QW and barrier layers which in turn inhibits phonon flow. The next section shows the detailed explanation. QW effects become significant only when the thickness of the active layer is small, i.e., below about 200D. The effectiveness of QW confinement and its effect on the figure of merit depends on many factors such as the carrier concentration, which is temperature dependent.

In addition to QW confinement, improvement in Z may result from the periodicity of the multiple film structure on the thermal conductivity *[1]*. At low values of the thickness of individual layers, there may be interference with the propagation of phonon modes, and therefore a reduction in 6_L. The theory of this effect, and its application to both in-plane and cross-plane thermal

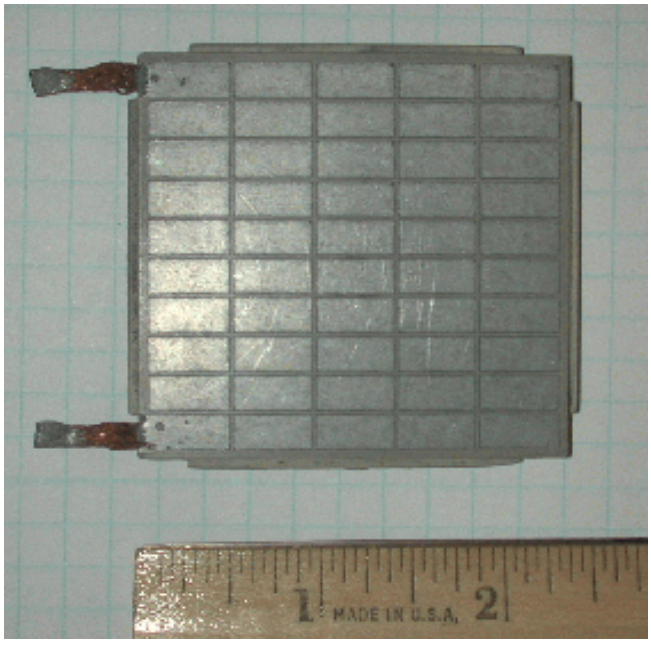

Figure 1. Hi-Z Thermoelectric Module

conductivity values, is now a subject of intense research and may evolve into a field of engineered thermal transport independently of thermoelectricity *[2&3]*.

Nomenclature

A	amperes	"	Seebeck coefficient
D	angstroms	6	thermal conductivity
k	kilo (10^{+3})	D	resistivity
m	milli (10^{-3})	S	ohms
M	matching factor	:	micro (10^{-6})
T_C	cold side temperature	W	watts
T_H	hot side temperature	V	volts
T	mean temperature	Z	figure of merit

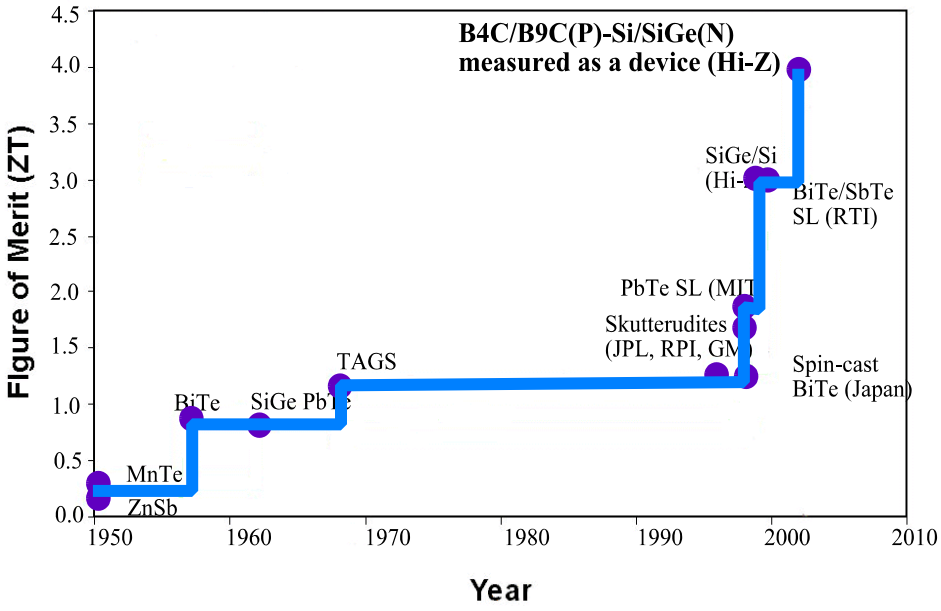

Figure 2. ZT Time Line.

Recent Advances

Hi-Z currently uses conventional Bi_2Te_3 alloy thermoelectric modules, as shown in Figure 1 *[4]*. The material in these modules has a value of ZT (figure of merit Z, times its mean absolute operation temperature T) of about 1. As shown in Figure 2, the value of ZT has hovered around 1 since the mid-1950s when semi-conductor materials were introduced into thermoelectric conversion. In the late 1990s new materials, including quantum well materials, were developed and a value of 4 has been achieved with B_4C/B_9C and with some promise that even higher values can be obtained as development continues.

The figure of merit (Z) for a thermoelectric material is obtained from its electric and thermal properties by

$$Z = \text{"}^2 / (\text{D} \cdot 6)$$

where " is the Seebeck coefficient of the material, V/K, D is its resistivity, ohm-cm, and 6 is its thermal conductivity, W/cm K. Efforts to improve the value of Z for a bulk material often fails because as one increases ", the values of D and/or 6 usually also increase so that the resulting value of Z either remains the same or decreases.

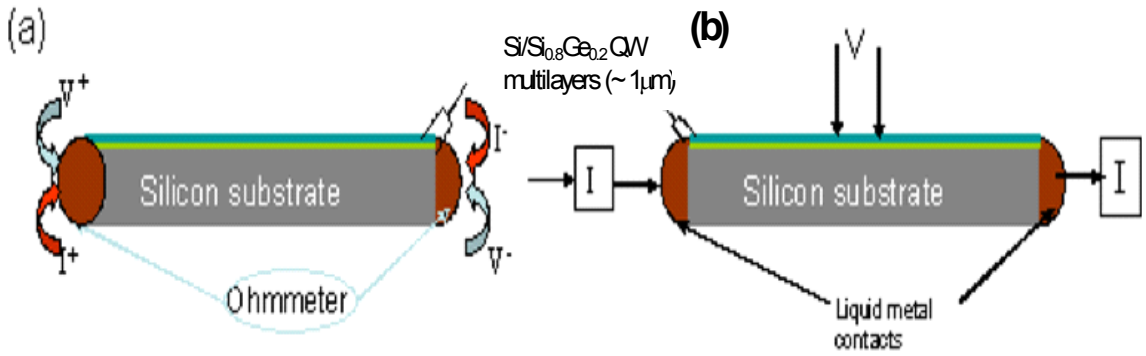

Figure 3. Schematic of the Measurement Setups for Obtaining the Resistance (D) of the Si/SiGe Multilayers on Si substrates using: (a) two-terminal Ohmmeter (Tegam Inc.) Probes, an (b) a four probe arrangement, where the current is sent through the liquid metal contacts at the ends while the voltage is measured along the sample with two more probes. Note: Typical design is grown to 8-10 :m of Si/SiGe multilayers.

Table 1 shows the measured thermoelectric property of Hi-Z QW samples, while Figure 3 shows the measurements setup. For this recent low resistivity QW thermoelectric sample, also measured by UCSD, and observed by NIST using the Hi-Z facility. Two measurements for electrical resistivity are shown: the two probe technique that includes the InGa electrical contacts and QW film while the second approach, the 4 probe technique allows the film resistivity to be measured because it is independent of contact resistance. It is not obvious why this specimen is exhibiting such a low 4 probe resistivity value although special efforts were made to improve the wetting of the liquid metal InGa contacts. Additional samples are being prepared to determine if the results can be obtained on multiple samples. NIST will further confirm the measurements using their measurement systems in the future.

Hi-Z has performed thermal conductivity measurements of QW films in the past using the most reliable technique, the 3-T method, and these measurements support the large reductions in the 6 of these thin films. Such measurements are very difficult to conduct and further thermal measurements such as efficiency and 6 are planned with these low resistivity films. When additional data become available, Hi-Z will start using the lower QW thermal conductivity value in the analysis. Table 1 also shows typical Bi_2Te_3 data for comparison.

Si/SiGe QW Thermoelectric

The thermodynamic efficiency, O, of a thermoelectric power generator is given by

$$\eta = \frac{M-1}{M+\frac{T_c}{T_h}} \times \left(1-\frac{T_c}{T_h}\right) = \frac{M-1}{M+\frac{T_c}{T_h}} \times \eta_{Carnot} \qquad (1)$$

where M is defined by

$$M = [1+Z(T_c+T_h)/2]^{1/2} \quad (2)$$

with T_h and T_c the absolute temperature of the hot and cold junctions respectively. To achieve a high efficiency, the figure of merit, Z, must be high.

For a specific material,

$$Z = F"^2/(6_L+ 6_e) \quad (3)$$

where F is the electrical conductivity, " is the Seebeck coefficient, 6_L is the lattice or phonon contribution to the thermal conductivity and 6_e is the electron contribution to the thermal conductivity. Note that the term to the right of Equation 1, is Carnot efficiency, which only has values between zero and one, so the "0" is always a fractional multiplier of Carnot efficiency.

Table 1. Performance of P-type Si/SiGe QW films. Recent Hi-Z Seebeck coefficient and electrical resistivity data, confirmed by UCSD and observed by NIST using Hi-Z facility. Bi_2Te_3 bulk alloy data is shown for comparison.

	Measured Seebeck Coefficient a, mV/K	**Measured Electrical Resistivity r, mS-cm**	**Power Factor a^2/r mW/cmEK^2**
Typical former QW sample at room temperature	1100	1.0	1,210
Recent QW sample material Measurements confirmed by UCSD and NIST	1200 1200	0.8 (2 probe technique) 0.04 (4 probe technique)	1,800 36,000
Bi_2Te_3 Bulk Alloy	220	1.1	44

The breakthrough approach to increasing Z is to form compositionally modulated materials (*e.g.*, Si/SiGe), mainly by QW confinement of carriers (electrons and holes) in the active layers (SiGe) in a multilayer film by adjacent barrier layers (Si). The core concept is to enclose each electrically active layer by a material which has a band offset sufficient to form a barrier for the charge carriers. The major improvement in Z is expected to follow from an increased Seebeck coefficient that results from an increase in the density of states from bulk (3D) to two dimensional (2D) quantum confinement. There is also a significant effect on the electrical and thermal conductivities due to quantum confinement, so ideally there would be improvement in Z from the ", F, and 6 terms of equation 3. QW effects become significant only when the thickness of the active layer is small, below about ~200D. In simple terms, QW effects are caused by quantum confinement which means, the carriers (electrons and holes) are confined in two dimensions as compared to the bulk material where the carriers are moving in three dimensions. The reduction in the dimensions of movement reduces the scattering centers of the carries, therefore the mobility is increased which makes the electrical conductivity (F) increases. We have measured the mobility of the samples which show this

enhancement. That increases the Z, which in turns increases the efficiency. The confinement reduces the thermal 6, since the wavelength of the phonons are larger than the electrons and holes. It has been shown experimentally and theoretically ~1/3 reduction in thermal 6 *[5]* of QW compared to bulk. It is this confinement in the QW (the two dimensionality) that increases the Z and then the 0.

The temperature dependent Seebeck coefficient is a function of the Fermi level and provides the basic information about the band structure and the density of states at the Quantum Well (QW) layers. From this information the observed Seebeck coefficients can be developed as described below. Additionally, information is provided about the various carrier scattering mechanisms.

The standard form of the electron dispersion in a QW layer is free electron like parallel to the layers, and tight binding like perpendicular to the layer,

$$E(k_{\parallel},k_{\perp}) = \frac{\hbar^2 k_{\parallel}^2}{2m_*} + t(1-\cos k_{\perp} d)$$

where m_* is the conduction band effective mass, t is the transfer integral (half the bandwidth) in the perpendicular direction, and d is the QW layer period. The density of states corresponding to this equation is:

$$n(\epsilon) = \frac{m}{\pi^2\hbar^2 d} \times \begin{cases} \cos^{-1}(1-\epsilon/t) & \epsilon<2t \\ \pi & \epsilon>2t \end{cases}$$

At temperature of absolute zero, impurities introduced by uniform or modulation doping yield carriers which fill the density of available states. For partial filling of the lowest miniband, the carrier density N corresponding to a Fermi energy E_F is:

$$N = \frac{mt}{\pi^2\hbar^2 d}\left\{-(1-\frac{E_F}{t})\cos^{-1}(1-\frac{E_F}{t}) + \left[2(\frac{E_F}{t})-(\frac{E_F}{t})^2\right]^{1/2}\right\}$$

The Seebeck coefficient (") would then be:

$$\alpha = \frac{\pi^2}{3}k_B T\left[\frac{1}{n(\epsilon)}\frac{\partial n(\epsilon)}{\partial\epsilon} + \frac{1}{v^2}\frac{\partial v^2}{\partial\epsilon} + \frac{1}{\tau(\epsilon)}\frac{\partial\tau(\epsilon)}{\partial\epsilon}\right]_{\epsilon=F_F}$$

where $n(\epsilon)$ is the density of states, v^2 is the square of the electrons velocity in the direction of external temperature gradient averaged over the Fermi surface $\epsilon = E_F$, and $\tau(\epsilon)$ is the energy-dependent momentum relaxation time.

Therefore from the above equation the change in Seebeck coefficient due to the effect of the thin film on the density of states could be written as:

$$\Delta\alpha = \frac{k_B}{e}\left\{\frac{(E_g - E)}{k_B T} + 1 + \left[2 - (\frac{E_g}{k_B T})(\frac{I_0^2}{I_1^2})\right] H\right\}$$

where E_g is the effective gap of the QW, therefore:

$$E = K_B T ln(\frac{\pi\eta^2 n_e d}{m k_b T})$$

and

$$H = \frac{[1 + (eE_0 d\tau)^2]}{[1 + 2eEd\tau)^2]}$$

where I_0, and I_1 are the modified Bessel functions of the argument $E_g/k_B T$.

The expression for) " can further be simplified for the special case where $k_B T > E_g$:

$$\Delta\alpha = \frac{k_B}{e} \ln(\frac{T}{t})$$

where ***t*** is a characteristic coefficient which depends on the QW layers. Therefore:

$$\alpha_{QW} = \alpha_{Bulk} + \Delta\alpha = \alpha_{Bulk} + 86 \times \ln\frac{T}{t}, \ with \ units \ of \ (\mu V/°C)$$

For Hi-Z typical samples this generated the curve in Figure 4. The theoretical data match the experimental data very closely. This excellent match between the analytical and experimental data makes the model very viable for understanding the " behavior.

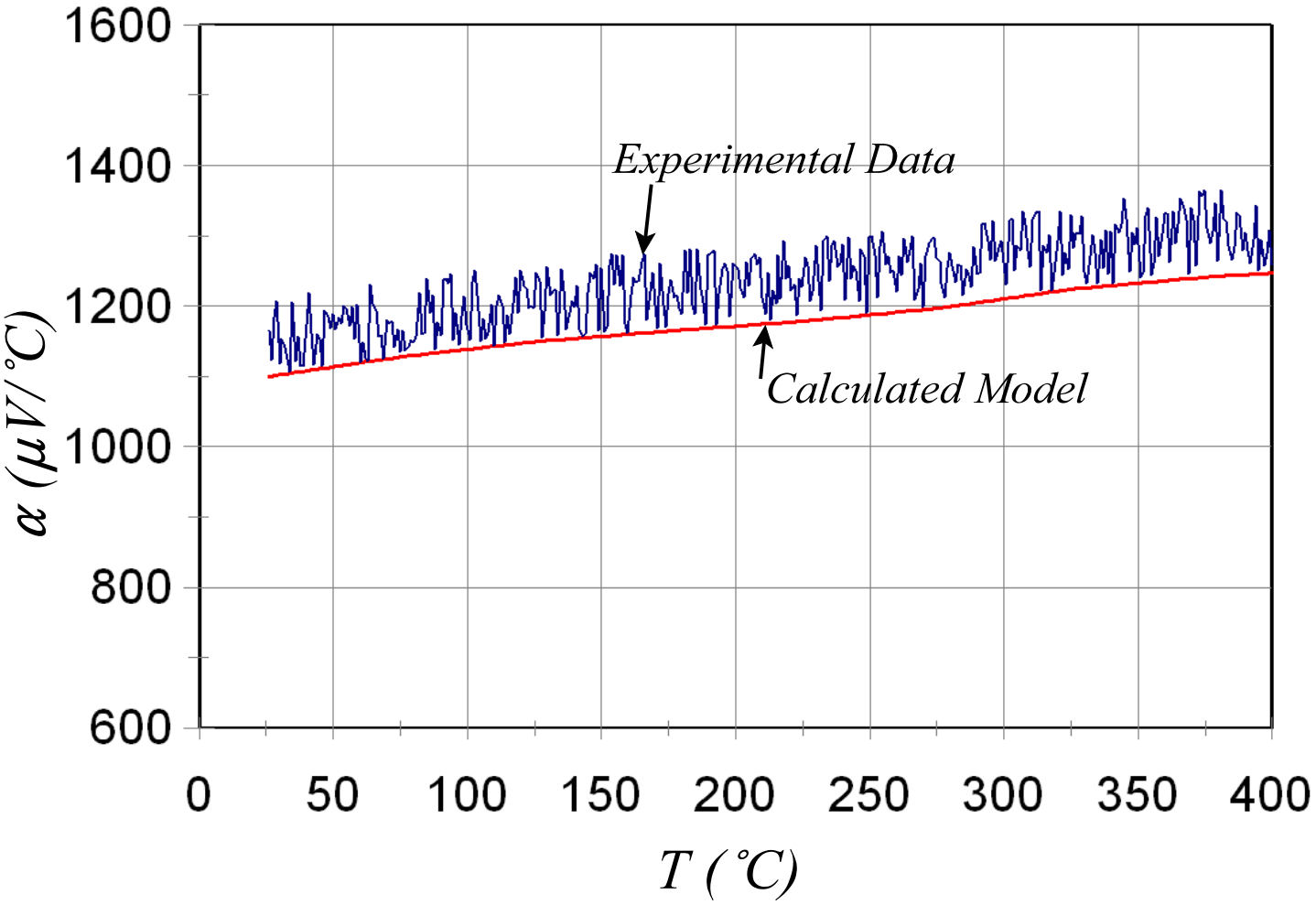

Figure 4. The Seebeck Coefficient versus Temperature. The calculated model matches the experimental data very closely.

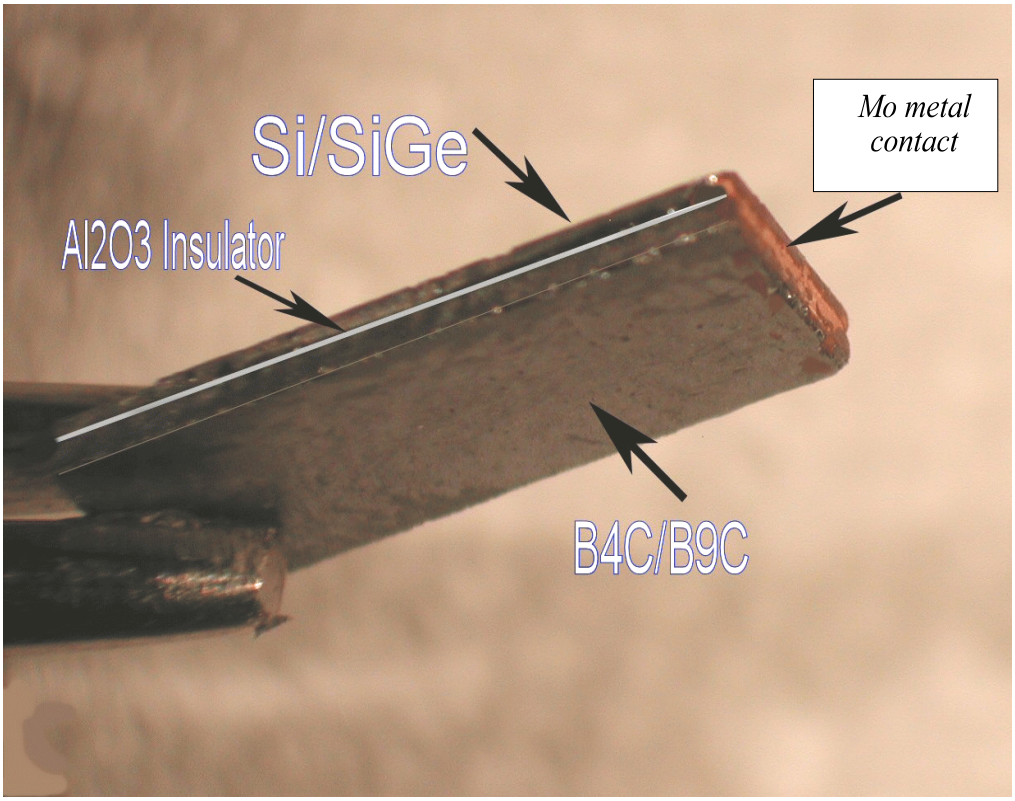

Figure 5. QW Si/SiGe-B_4C/B_9C couple for thermal stability test (0.2" x 0/8"). The Mo was deposited by an improved sputtering process. This is the first couple where an Al_2O_3 insulator was used (0.01" thick). The initial power generated agrees closely with that calculated from property data for the N and P materials.

QW Thermoelectric Device Life Test

Figure 5 shows a QW couple with B_4C/B_9C and Si/SiGe. An improved sputtering process was successfully developed to deposit the Mo metal contacts that exhibit a negligible contact resistance with both N and P material.

This QW couple was fabricated for life testing with N type Si/SiGe and P type B_4C/B_9C and operated for ~4,000 hours in a fairly stable mode and then degraded sharply to zero power the last few hundred hours, as shown in Figure 6. At cool down the N and P legs were no longer electrically connected. The ~2 mm thick Mo that joined the N and P legs on the hot side was not distinguishable. It may have fallen off the surface of the couple in its removal from the chamber and was lost.

Each leg was measured for " and r and essentially both legs remained constant in thermoelectric properties as shown in Table 2 indicating the degradation problem is all in the joint area.

The N leg of Si/SiGe QWs and the P leg of B_4C/B_9C were examined on the SEM on cross section as shown in Figures 7 and 8. As can be seen the Mo was well bonded to the Si and SiGe layers in some areas while in other areas failure occurred primarily in the Si/SiGe right next to the interface, possibly due to thermal cycling or some of the Si/SiGe layers might have had microcracks

induced during preparation of the sample that propagated during life testing and/or during periodic thermal cycling to room temperature to measure " and r, caused high thermal stresses. In future life testing the thermoelectric properties will be measured with the N and P couple at temperature.

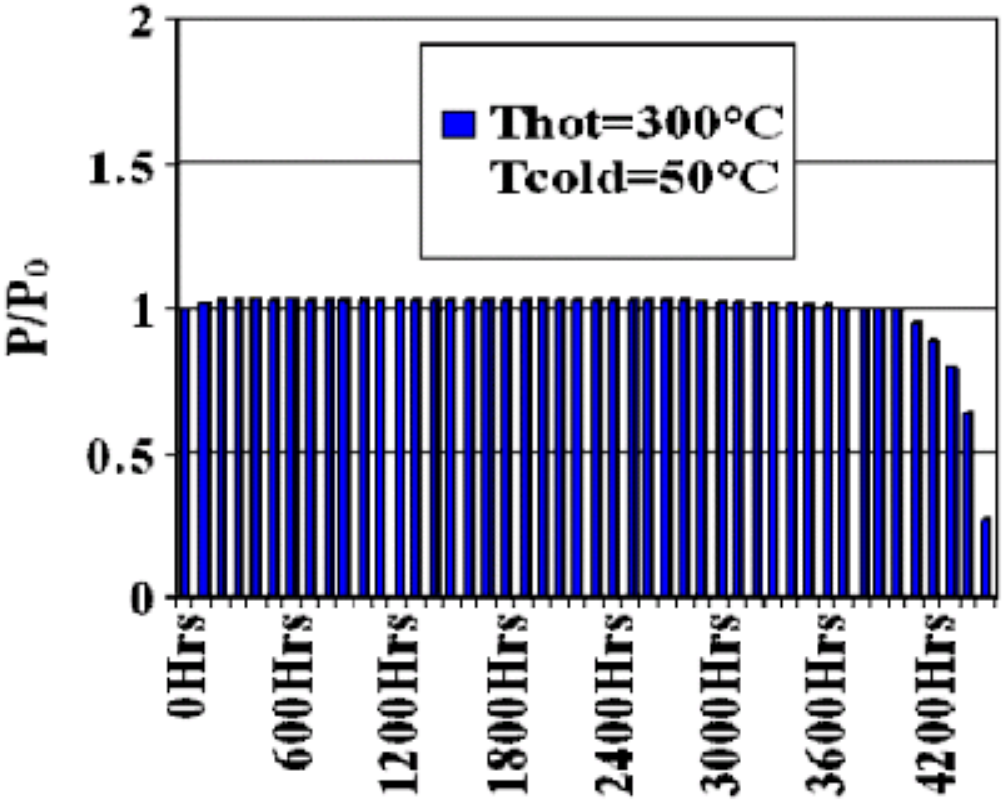

Figure 6. Life Test Data.

Table 2. Measurements of Si/SiGe and B_4C/B_9C Legs Before and After Gradient Testing for ~4300 Hrs.

	Seebeck before aging	**Seebeck after ~4,300 hours aging**	**Resistivity before aging**	**Resistivity after aging**
Si/SiGe leg	~ -1260 mV//C	~ -1220 mV//C	~ 1.05 mS-cm	~ 1.1 mS-cm
B_4C/B_9C leg	~ +1120 mV//C	~ +1090 mV//C	~ 1.1 mS-cm	~ 1.2 mS-cm

Table 3. P type Si/SiGe Annealed at 1000/C, 24 Hours Showed no Significant Change in Seebeck Coefficient and Electrical Resistivity.

	Seebeck Coefficient mV//C	**Electrical Resistivity mS-cm**
Before	~1000	0.75
After	~1000	0.76

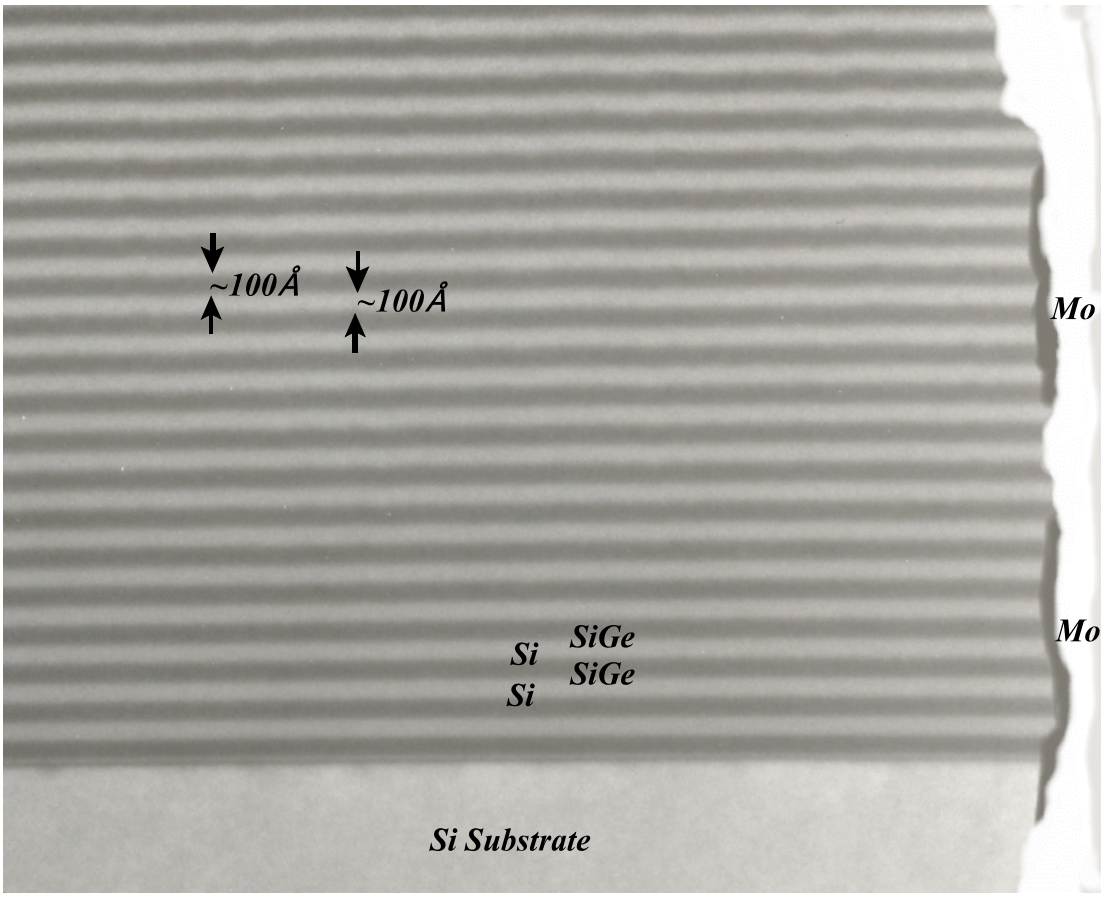

Figure 7. 150kX SEM of Si/SiGe leg of the ~4000Hrs aged couple.

It was known before testing that thermal expansion differences among most of the components were quite small. However, the B_9C is known to be higher and may also initiated cracking during periodic thermal cycling. Future couples will have much thicker Mo than the ~ 2mm of Mo on this couple to provide more strength and not be as easily embrittled by diffusion of SiGe, B or C into the Mo.

Thermal Stability

A single crystal Si substrate coated with Si/SiGe QW films was subjected to a 24 hour anneal at 1000/C. The before and after Seebeck coefficient (") and electrical resistivity (r) both before and after anneal is shown in Table 3 and indicates little or no change in thermoelectric properties. Previous longer term anneals, up to 600/C, also indicated no change in thermoelectric properties.

From all the isothermal and gradient thermal stability tests conducted thus far, there is no indication that these Si/SiGe QW films will degrade during operation as shown by the gradient data and the 1000°C-24 hours isothermal data shown in Table 3.

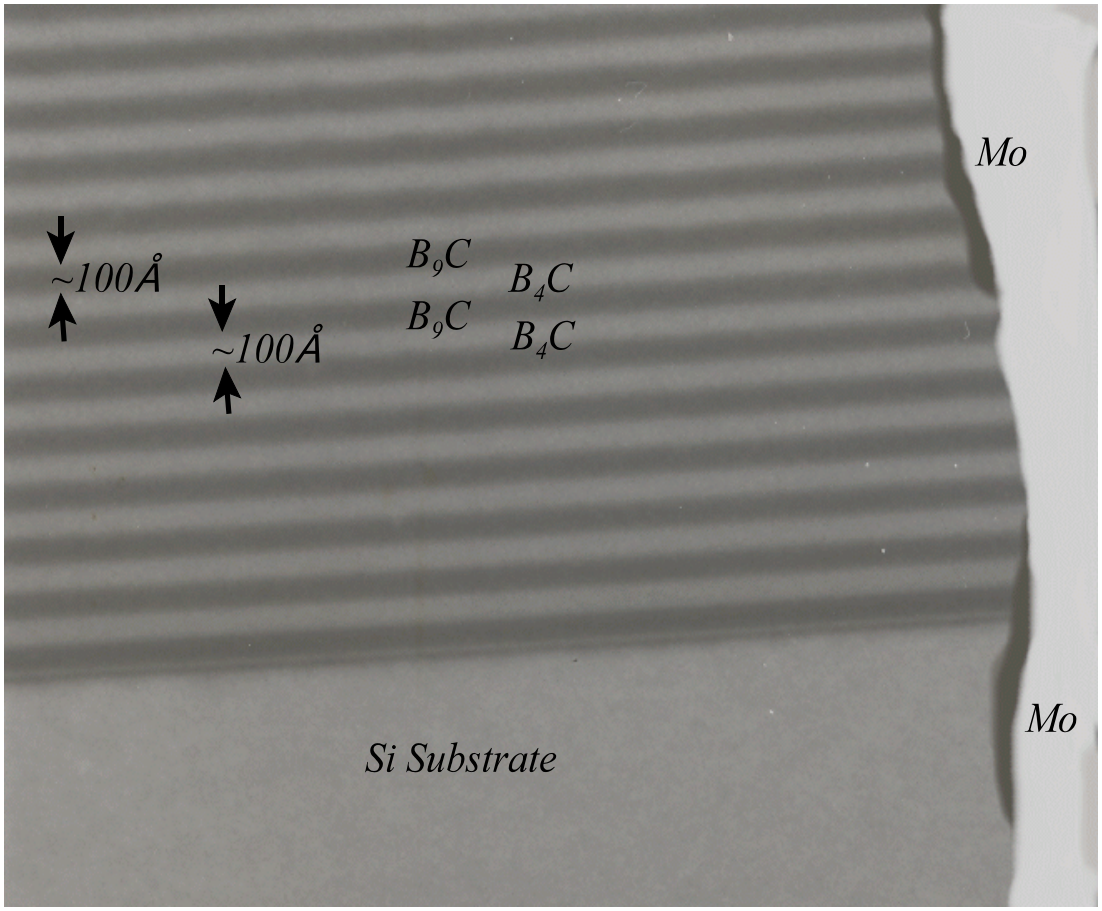

Figure 8. 150kX SEM of B_4C/B_9C leg of ~4000Hrs aged couple.

Highest Potential Thermoelectric Efficiency

New verified materials data , presented on the last section, indicates predicted thermoelectric module efficiencies of greater than 30% at a hot side temperatures greater than 300/C and greater than 40% at hot side temperatures greater than 400/C (see Figure 9). With such results, solid state thermoelectrics can compete with gasoline, diesel, turbine, *etc.*, engines.

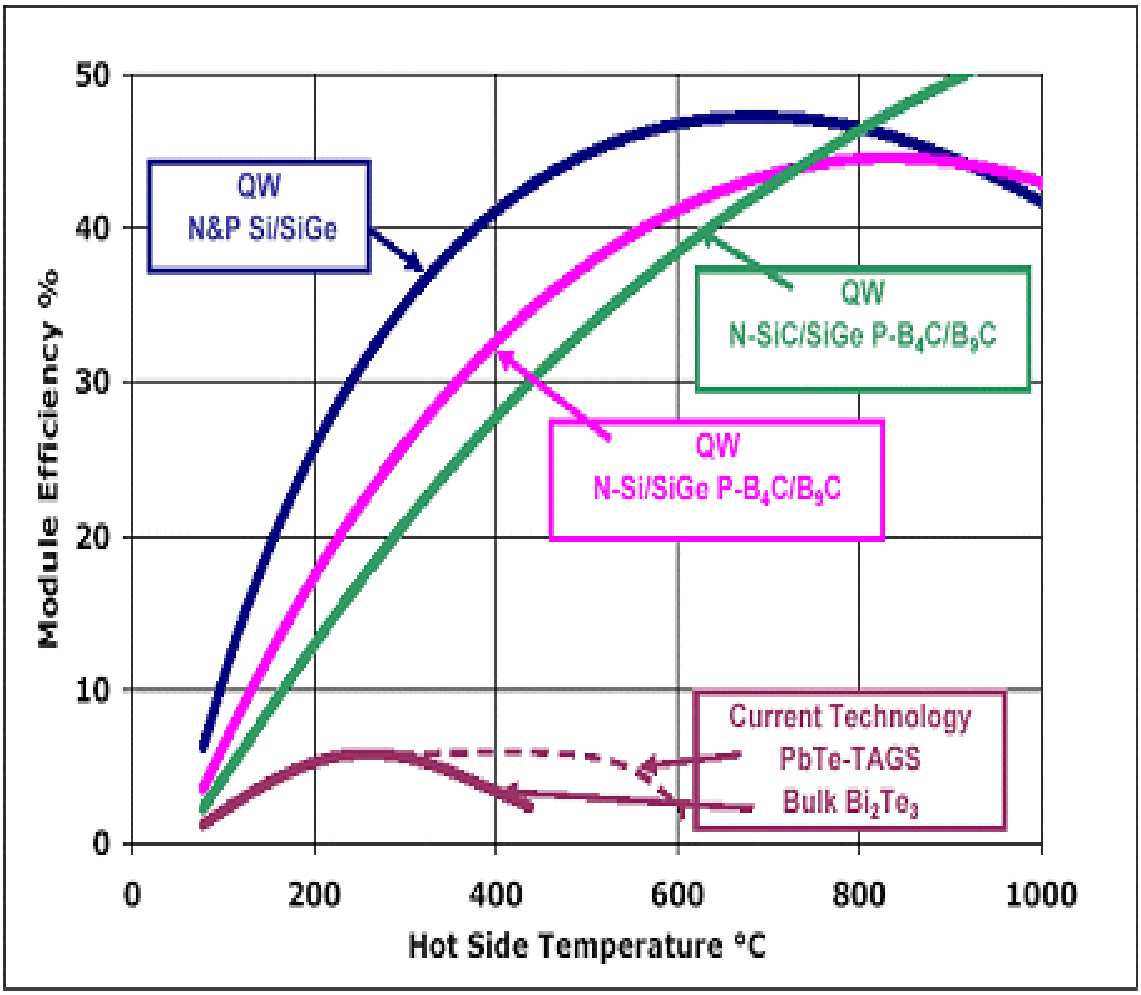

Figure 9. Predicted Efficiency of Quantum Well (QW) thermoelectric modules using recent Seebeck coefficient and electrical resistivity data, " and ρ, for QW Si/SiGe. Verified by UCSD (12/2006) and NIST (3/2007). To be conservative, electrical resistivity of QW Si/SiGe is increased according to slope of prior data causing efficiency to decrease at very high temperatures; and published literature bulk thermal conductivity of Si/SiGe is used for determining the Figure of Merit, Z = " ^{2}/ρ6. Expected thermal conductivity, 6, is 1/3 of bulk 6, which results in an even higher efficiency. Cold side at 50/C. Substrates are 50 μm thick 50% porous Si, with 3 μm single crystal Si on the film side.

Quantum well performance predictions use a 50% porous Si. There are several pertinent published reports on investigations of the thermal conductivity of porous Si (Refs. 4-10) for electronics applications. Reported data shows that porous Si has a thermal conductivity 2 to 3 orders

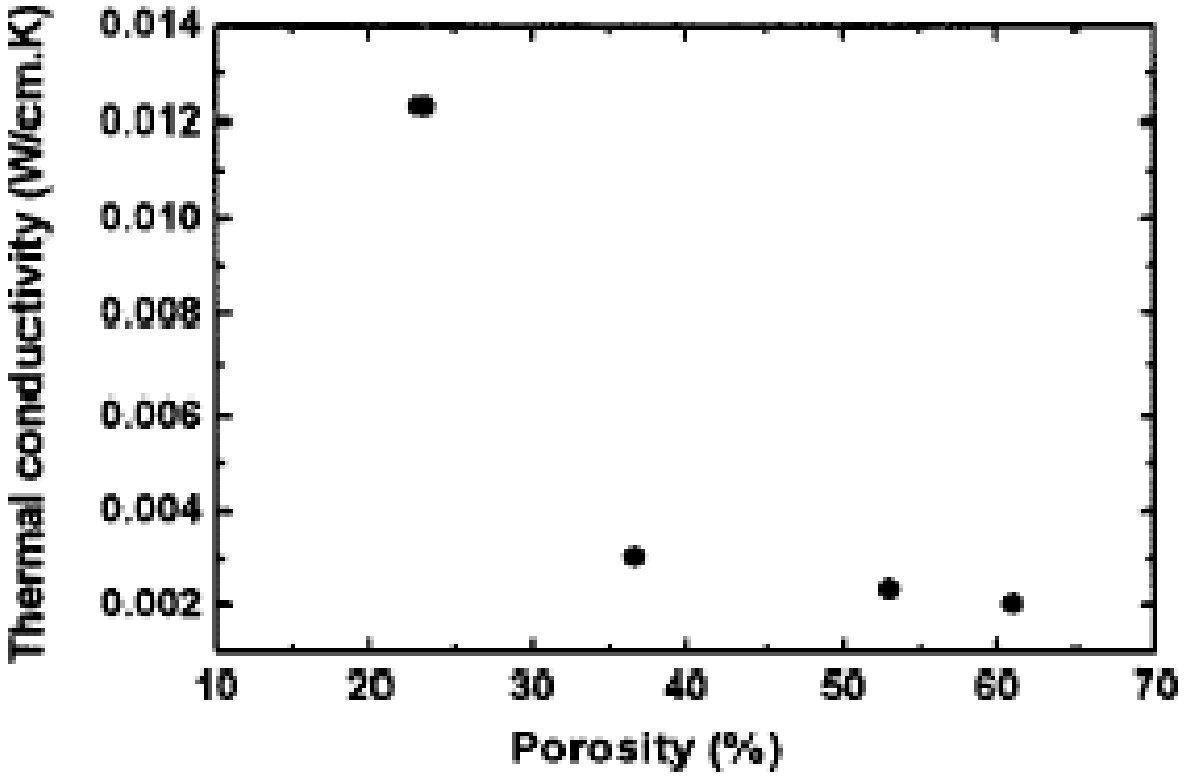

Figure 10. Dependence of thermal conductivity 6 of the film on its porosity showing large reduction compared to single crystal Si at 1.4 W/cmEK which is not shown above.

of magnitude lower than a single crystal Si and approaches that of Kapton. An example of published data by Shen and Toyoda (Ref. 8) is shown on Figure 10.

Joining and Electrical Contacts

During the late 1960s and early 1970s when the bulk SiGe alloys were being developed and scaled up to eventually operate at a T_H of 1000/C, electrical contacts were being developed and extensively tested for space power applications. In fact these generators which were launched in 1976 are still functioning today outside the Solar system. Early workers used Mo and W contacts but were limited to <600/C because the metals would silicide and increase in resistance due to volume changes at the interface. The result was a composite of $MoSi_2$ plus a little Si to modify the alloy's coefficient of thermal expansion so it was the same as $Si_{0.8}Ge_{0.2}$. The material is compatible with SiGe alloys because no further reactions occur at the higher temperature.

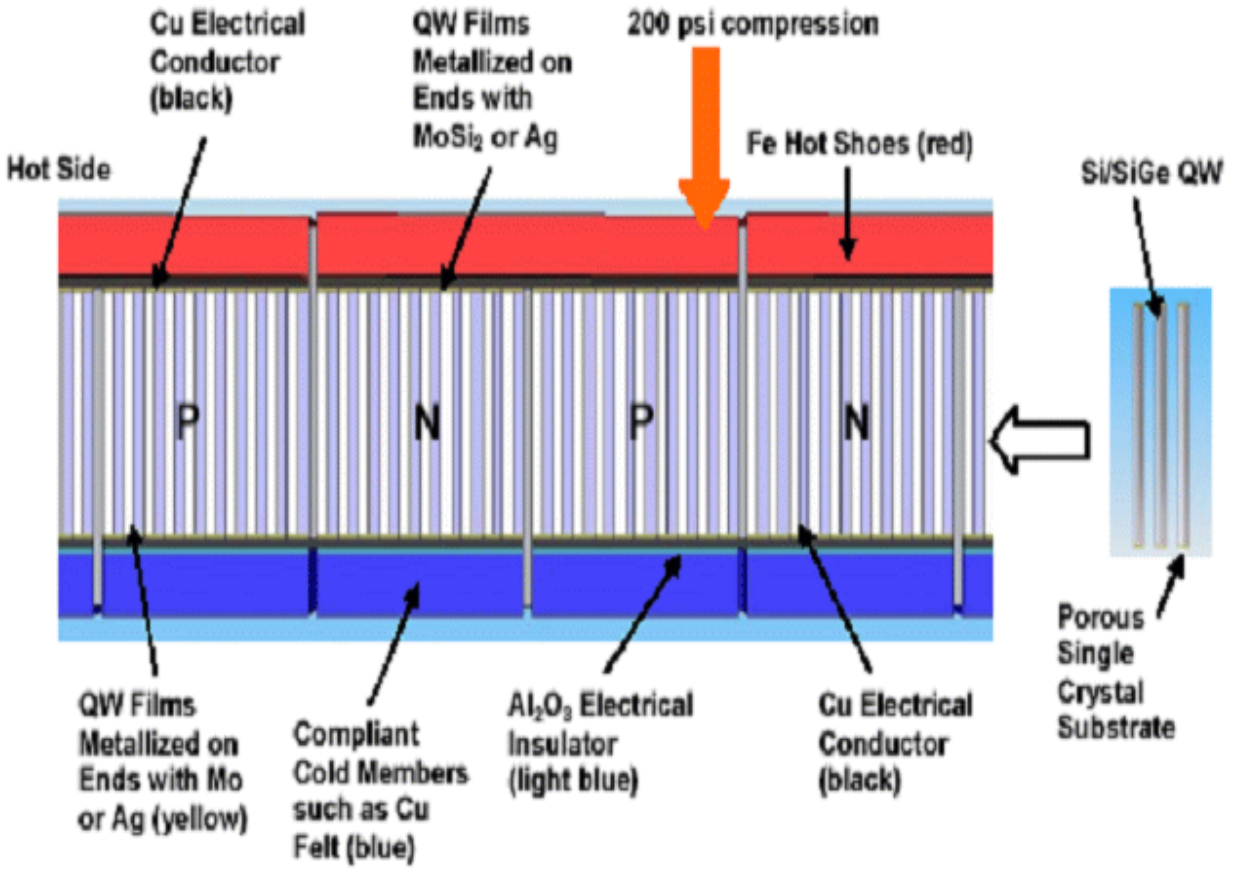

Figure 11. Schematic Showing Two N and P Couples in a Quantum Well Module. Each leg consists of ~100 layers of 11 μm Si/SiGe on 1μm Si buffer layer on 50 μm Si substrate (see Fig. 3). The assembly is based on prior PbTe work where this design provides excellent thermal contact with compliant members and will allow a large number of thermal cycles for power and cooling modules.

Besides $MoSi_2$, dense graphite that shows a minimum reaction with SiGe also demonstrated encouraging performance in extensive life testing at 1000/C. Ag and AL are also candidates for the <300/C operations. Both elements are used as contacts with PV cells.

This information could be used as follows. Up to ~500/C, Hi-Z will continue to pursue Mo and W contacts for the N and P type Si/SiGe alloys based on the past extensive RCA and Sandia studies. Also, up to 500-600/C Hi-Z will evaluate Ag and Al as a contact material. RCA did not have this option because of their couple/generator design. Ag is unique in that it does not form a silicide, or tenacious oxide film like Al, is very ductile at all temperatures and when used in compression as shown in Figure 11, it should be compliant during thermal cycling.

QW TE Applications

Energy Harvesting From Small Temperature Differences

Quantum well devices are suited for compact applications since a single N leg or P leg with 1100 ten nm films is only 11 microns thick on a 5 to 25 micron substrate, and the voltage for this couple is five times larger than a couple made with today's Bi_2Te_3 alloys. An example of a module design concept is shown in Fig. 12. This module will produce 5 mW of electrical power and an open circuit voltage of 6 V with a 40/C DT. The module is in the form of a flat disk. It contains 26 semi-radial QW film legs with the N type Si/SiGe film deposited on one side of the substrate and P type Si/SiGe film on the other. These legs are made by depositing the film through a mask. The legs consist of multiple 100Å thick layers. Electric connections can be made by either depositing metal on the inner and outer edges of the disk or by plating through hole at each end of each leg. Some applications require a much larger number of legs, which are typically narrower than shown in Fig. 13, and for such a case it may be preferable to use two or three sub-modules for the ease of manufacturing and making of electrical connections. The sub-modules can be stacked to provide higher voltage and power for radial or axial heat flow applications.

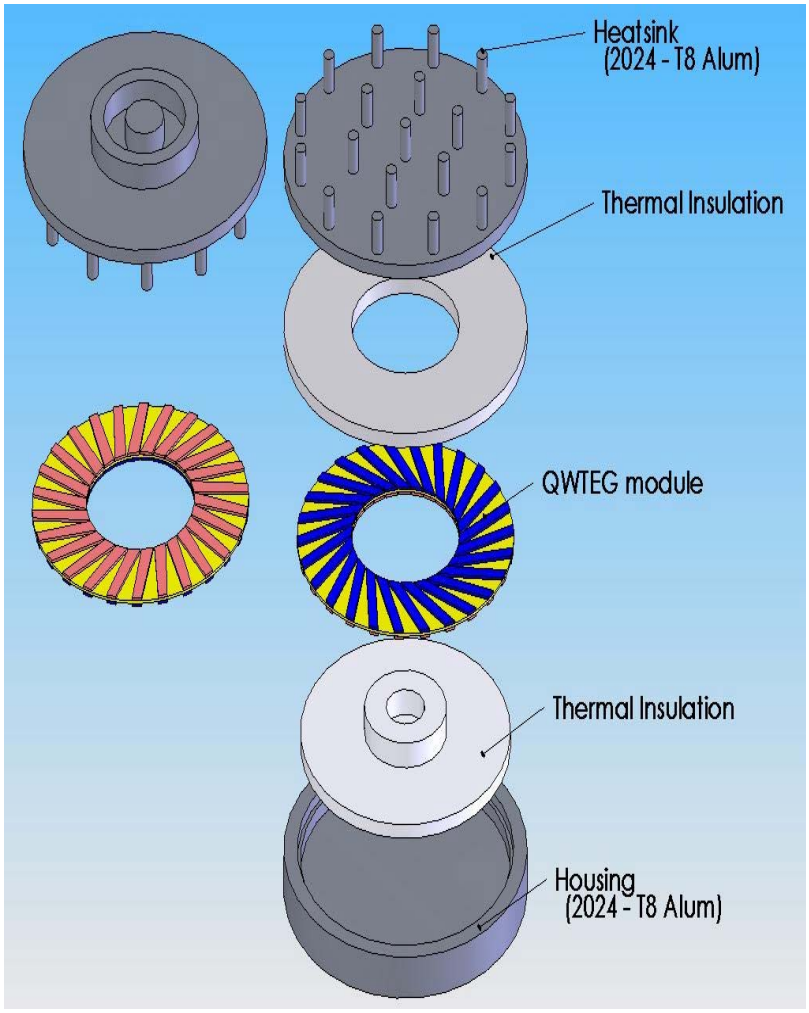

Fig. 12. Components of the quantum well electric generator. Diameter is 1 inch.

The main heat flow through this generator system is in the bottom and up the side, radially inward through the QW TEG module, up the center post to the heat sink above the module and into the pin fins where it is dissipated to the ambient air. A nylon screw is used between the bottom hot surface and the heat sink in order to minimize the bypass heat loses. A thin support tube, made of Vespel, or similar thermally insulating material, is used to separate the heat sink of the hot surface at the outer boundary in order to minimize the thermal bypass losses and to contain the internal thermal insulation.

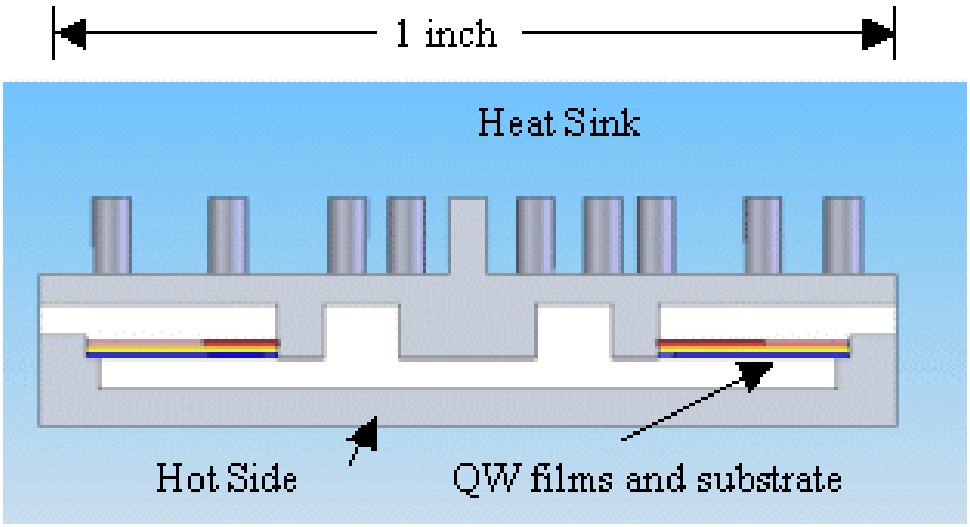

Fig. 13. Assembled components of the quantum well generator with radial heat flow for one inch diameter generator shown on Fig. 12.

High Power Quantum Well Thermoelectric Generators

A typical arrangement of Hi-Z's quantum well thermoelectrics is in a cylindrical arrangement for an industrial stack, engine exhaust, or producer gas application such as shown in Fig. 14. Since each quantum well module is flat, the modules could also be used as a refractory brick or heat exchanger section replacement. Thermoelectric power depends on the temperature difference across the thermoelectric module, and the "cold side" can be water, hot oil or air (forced or natural convection). With quantum well materials measured high temperature capability, water can be heated on the "cold side", near 100/C, to provide a source of hot water.

Predicted voltage and efficiency, based on quantum well measured material properties, for a typical single module, are shown on Fig. 15. This module is 2.35 in. x 2.35 in. square x 0.50 in. thick (same footprint as Hi-Z's HZ-14 commercial module) and at the expected heat flux of 18 W/cm^2 produces ~70 W_e. For instance, to obtain one kW_e of power, 13 modules can be arranged in series. Another powerful method to improve power output is to utilize the high temperature available in the waste heat stream. Many applications have temperatures >700/C. Assuming a 200/C drop across a fluid film (measured in vehicle exhaust) the hot side of the thermoelectric could run at 500/C. A large increase in power is possible as shown in Fig. 16. Hi-Z needs to develop, design and fabricate a new high temperature module to realize these higher powers and efficiencies.

The thermoelectrics can easily be scaled in diameter and length to give more power. With quantum well materials, our predictions indicate that with hot gas at 500/C (300/C at thermoelectric hot side and 100/C at the thermoelectric cold side) in a 5 inch flow path, a 5 kW_e generator can be packaged with 64 quantum well modules in a 30 in. long section with a 10 in. outside diameter. For

use on a waste heat stream, the modules are loaded as shown in Fig. 17 between the finned hot side, and a liquid cold side heat exchanger. The 64 quantum well thermoelectric modules are individually loaded and coolant heat exchangers are electrically arranged in a series or parallel circuit. The heated coolant can be used for heating, sanitation or hot oils for cooking.

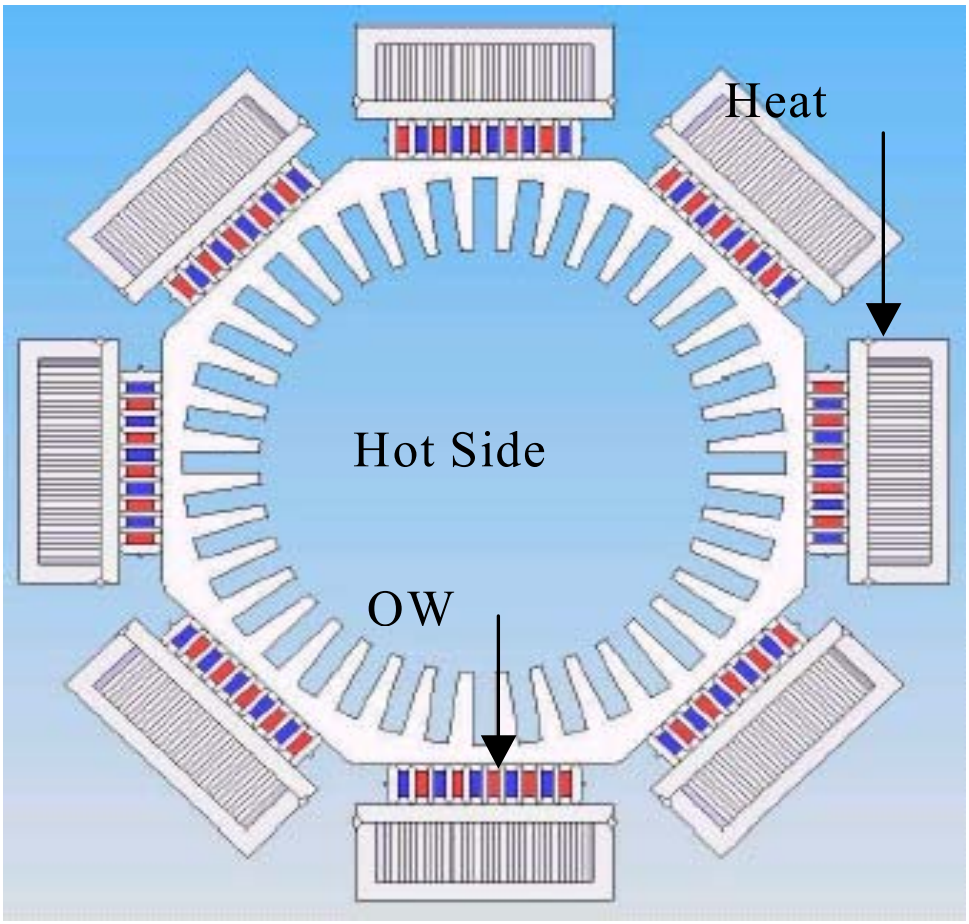

Fig. 14. Cross section through hot waste heat exchanger, quantum well modules and liquid heat sinks. Outside diameter is 10 inches.

Costs

Current bulk thermoelectric power modules are predicted to cost somewhat less than $1/Watt when produced in high volumes. Similar quantum well modules are predicted to cost less than $0.35/Watt in large volume production. A detailed cost analysis has been completed for production of quantum well modules. The cost of cooling modules will be somewhat less on a per watt basis. The reason for the predicted lower cost of quantum well devices is due both to their higher efficiency [11-14] and the fact that they are made from lower cost raw materials than bulk thermoelectrics.

Hi-Z's current quantum well film production has been quite low because of the limitation of our laboratory equipment. Our current quantum well programs have allowed us to obtain a much larger sputtering machine. In addition, we are working with a large organization to peruse production scale-up of quantum well films. Hi-Z is also investigating alternative means to fabricate quantum well films at higher rates.

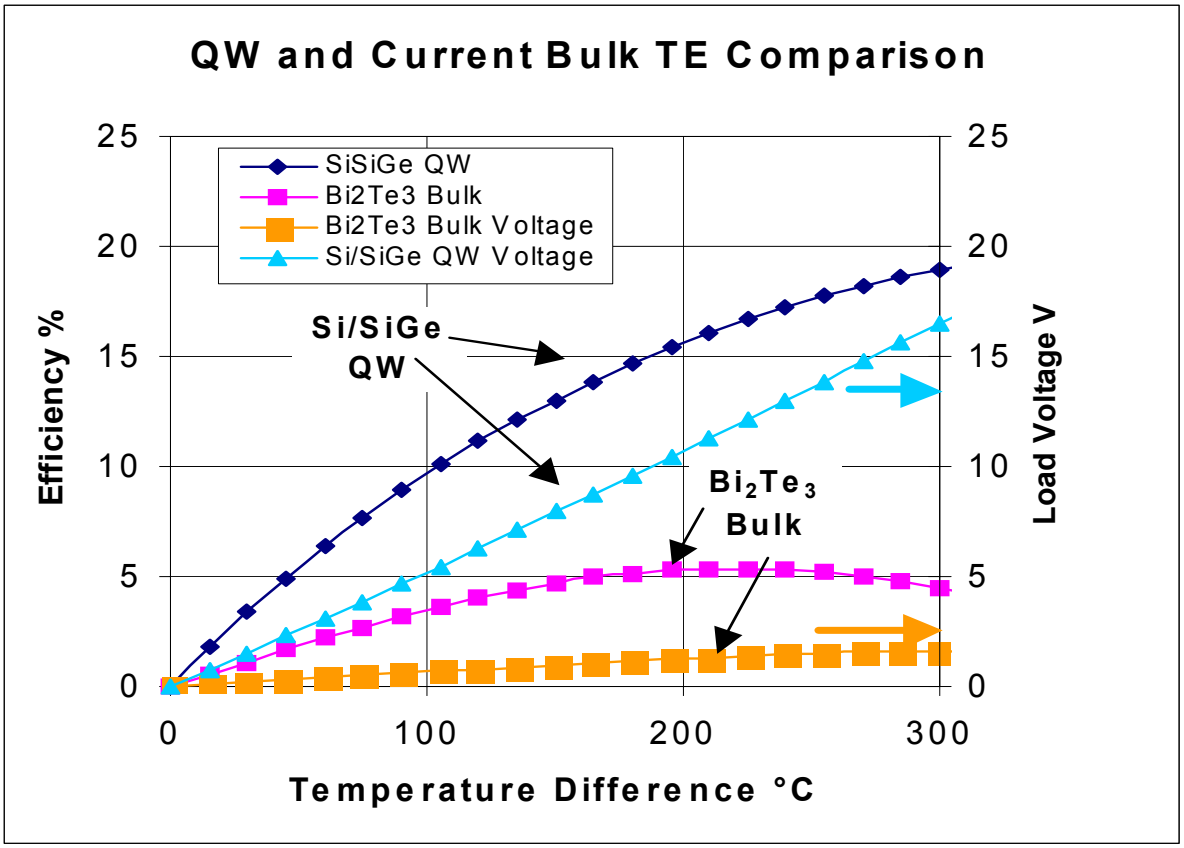

Fig. 15. QW TE Efficiency from most conservative (high ρ, bulk κ) data

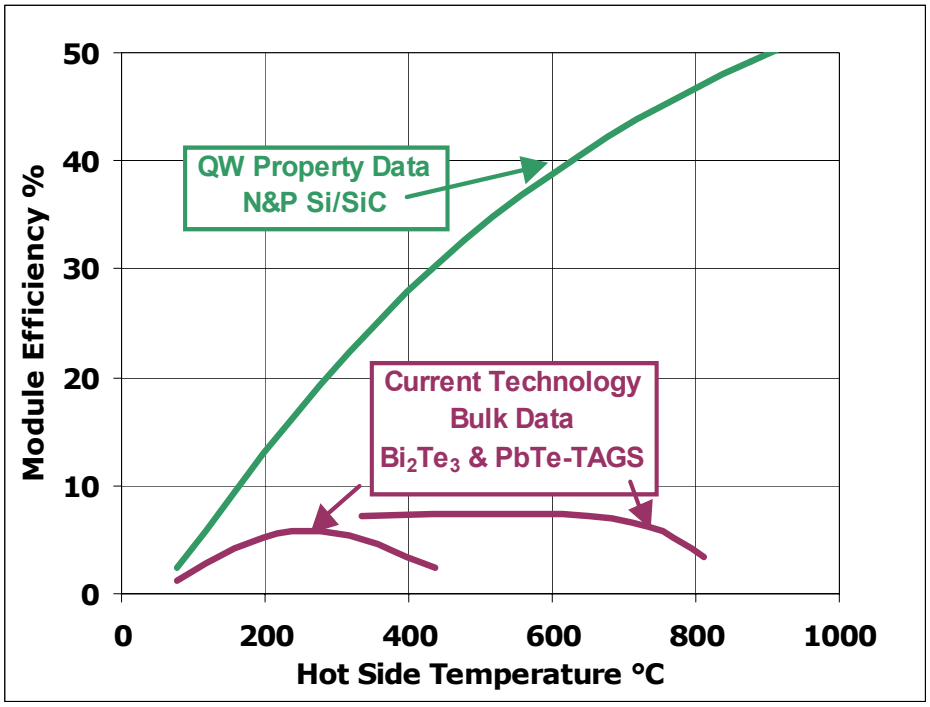

Fig. 16. Predicted efficiency of QW thermoelectric modules using measured Seebeck coefficient, ", and electrical resistivity data, ρ, for Si/SiC QW.

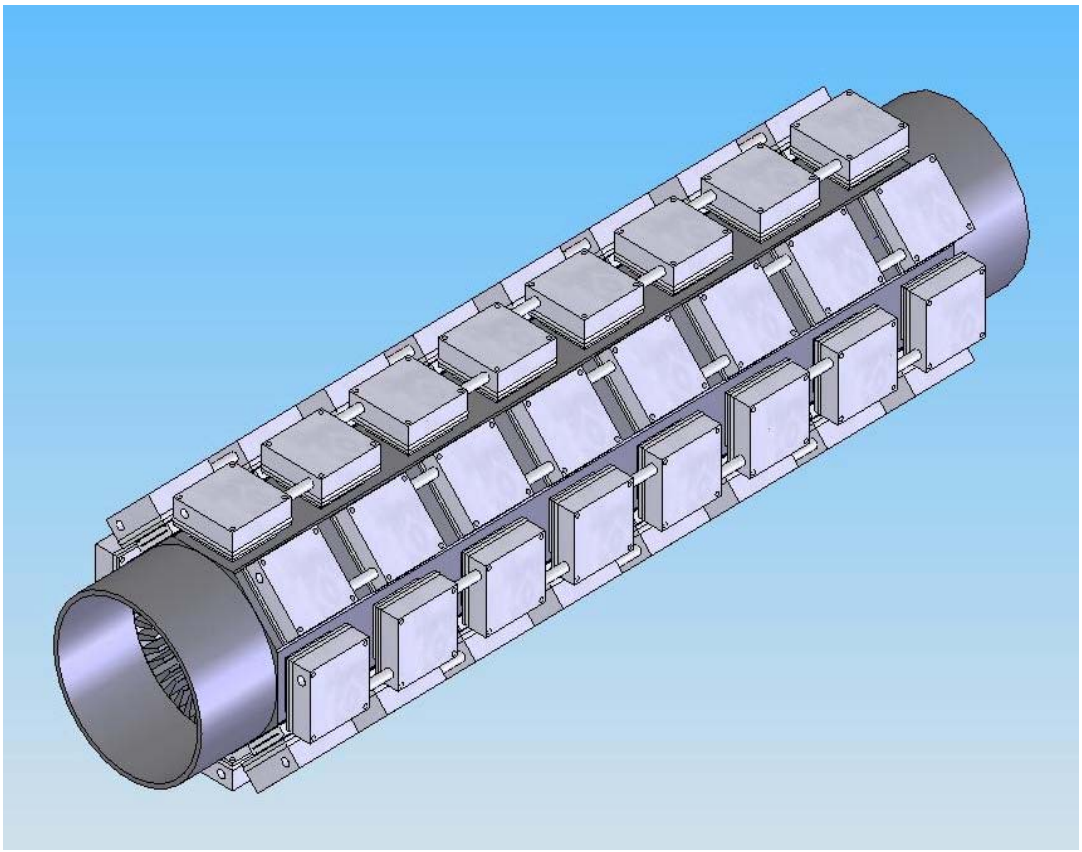

Fig. 17. Arrangement of 64 quantum well modules with liquid heat exchangers on 5 in. ID stack.

References

1. Harman, T.C., "PbTeSe/BiSb Short Period Superlattics as a New Thermoelectric Cooling Material," *Proc. 1st Natl. Thermogenic Cooler Conf., Center for Night Vision and Electro-Optics*, U.S. Army, Ft. Belvoir, VA, 1992
2. S. Ghamaty, N. Elsner, K. Wang and Q. Xiang, " Thermoelectric Performance of B_4C/B_9C Heterostructures" , ICT 1996, Pasadena, California.
3. Hicks, L.D., Dresselhaus, M.S., "Effect of Quantum-Well Structures on the Thermoelectric figure of Merit," *Phys. Rev. B.47*, 19 (1993) 12 727-731.
4. "Proof-of-Principle Test for the thermoelectric Generator for Diesel Engines", 1991, Final Report, Hi-Z Technology, Inc., HZ 72691-1.
5. Elsner, N.B., Ghamaty, S., Norman, J.H., Farmer, J.C., Foreman, R.J., Summers, L.J., Olsen, M.L., Thompson, P.E. and Wang, K., 1994, "Thermoelectric Performance of $Si_{0.8}Ge_{0.2}$/Si Hetrostructures by MBE and Sputtering", Proceedings, 13th International Conference on Thermoelectrics, AIP Press, Kansas City, MO.
6. Martin, P.M. and Olsen, L.C., 2003, "Scale-up of $Si/Si_{0.8}Ge_{0.2}$ and B_4C/B_9C Superlattices for Harvesting of Waste Heat in Diesel Engines", Proceedings, 9th DEER Conference, Newport, RI..
7. S. Ghamaty and N.B. Elsner, "Quantum Well Thermoelectric Devices", MRS, Boston, Mass., 2004.
8. Flinn, MRS Bulletin, Nov. 1995, pps. 70-73.
9. Ghamaty, S., 2002, "Quantum Well Thermoelectric Devices", Proceedings, DARPA/ONR/DOE High Efficiency Thermoelectric Workshop, Coronado, CA.
10. N.B. Elsner, " Review of PbTe Fabrication Techniques, MRS Vol. 234.
11. Energy use, Loss and Opportunity Analysis: U.S. Manufacturing and Mining, December 2004, Energetics, Inc., E3M, Incorporated, Table 11-3, page 73.
12. Hendricks, Dr. Terry and Choate, William T., "Engineering Scoping Study of Thermoelectric Generator Systems for Industrial Waste Heat Recovery", US. DOE, Industrial Technologies Program, (2006).
13. Chen, G., "Size and Interface Effects on Thermal Conductivity of Superlattices and Periodic Thin-Film Structures," ASME *Journal of Heat Transfer*, Vol. 119, No. 2, pp. 220-229.
14. Da Silva, A. Ferreira, *et al*., "Thermal and Optical Properties of Porous Silicon", *Materials Research*, Vol. 4, No. 1, 2 3 -26 (2001).
15. Li, D.Y., Wu, Y., Fan, R., and Yang, P.D., "Single Crystal Si Nanowires Can Not Conduct the Heat", *Appl. Phys. Lett*. 83, 3 86 (2003).
16. McGaughey, A. J. H., and Kaviany, M., "Thermal Conductivity Limits in Porous Crystals", *International Journal of Heat and Mass Transfer* (2 articles in press).
17. Theodoropoulou, M, *et al.,* "Transient and AC Electrical Conductivity of Porous Silicon Thin Films", *phys. stat. sol*. (a) **197**, No. 1, 279-283 (2003).